Norwegian University
of Life Sciences

Master's Thesis 2024 30 ECTS
Faculty of Environmental Sciences and Natural Resource Management

Exploring historical climate-growth relations in Norway spruce, across varying site conditions in southern Norway

Ruben Eik Birkeland
Forest sciences

Acknowledgments

The completion of this master’s thesis signifies the culmination of my five-year scholarly pursuit at the Faculty of Environmental Sciences and Natural Resource Management (MINA) at the Norwegian University of Life Sciences (NMBU).

First and foremost, I extend my profound gratitude to my primary and secondary supervisors, Line Nybakken (NMBU) and Danielle Creek (NMBU), for their amiable guidance throughout my master's thesis work, commencing with field work and concluding with the composition and drafting of this thesis.

Then I extend my gratitude to the team at CzechGlobe for hosting me in Brno and sharing their expertise in dendrochronology. Special thanks to Jan Světlík, Marko Stojanović, Soham Basu, and Sergei Mikhailov for their invaluable guidance and support in different facets of my work. I am also thankful to Tomáš Kolář for the many hours I was able to spend at the dendrolab and the facilities at Mendel University.

Lastly, I wish to acknowledge my fellow students for the myriad forestry-related and wonderfully peculiar conversations we have shared during my enriching years at NMBU.

Norwegian University of Life Sciences

Ås, 15th of May 2024

Ruben Eik Birkeland

Abstract

This study investigates the climate-growth relationships of Norway spruce (*Picea abies*) across a north-south gradient in Norway. The research encompasses ten forest sites spanning 325 kilometres from Stor-Elvdal (north) to Aremark (south), within the boreal and southern boreal vegetation zones. Tree-ring analyses of 125 trees revealed distinct regional differences in radial growth responses to temperature and precipitation.

From 1960 to 2022, mean temperatures significantly increased at all sites, extending the thermal growing season (TGS) by an average of 18 days. The most substantial warming trends occurred in the Mid and North regions, where average annual temperatures rose by up to 3°C. Precipitation trends varied, with mild increases in the South and Mid regions, while the North region remained relatively stable.

The climate-growth correlations revealed distinct regional patterns: in northern sites, June temperatures had the strongest correlation with Basal Area Increment (BAI), highlighting the thermal limitations of radial growth at these latitudes. In contrast, southern plots demonstrated a greater sensitivity to July precipitation, indicating more hydrological sensitivity. BAI analyses indicated a general stabilization or increase in growth in northern plots. Conversely, southern plots experienced a marked decline starting around 2010, persisting at least until 2019.

Overall, the results confirm that northern forest stands are primarily limited by temperature, whereas southern forests rely more on precipitation for growth. Thus, improving our understanding of where the boundaries between temperature and precipitation limitations lie. As average temperatures continue to rise, these constraints may shift, underscoring the importance of monitoring the impact on forest ecosystems. Understanding these regional differences in climatic sensitivity is crucial for developing adaptive forest management strategies in the face of climate change. Future research should incorporate a more holistic approach, utilizing additional data and extending the study to more sites and species to refine our understanding of climate impacts on boreal forests.

Sammendrag

Denne studien utforsker forholdet mellom klima og vekst hos gran (*Picea abies*) langs en nord-sør gradient i Norge. Studien dekker ti forskningsfelt som strekker seg 325 kilometer fra Stor-Elvdal i nord til Aremark i sør, innenfor den boreale og boreonemorale vegetasjonssonen. Årringanalyser fra 125 trær avdekker tydelige regionale forskjeller i trærnes vekstreaksjoner på temperatur og nedbør.

Fra 1960 til 2022 har det vært en signifikant økning i gjennomsnittstemperaturene over alle studieområdene, noe som har ført til en forlengelse av den termiske vekstsesongen (TGS) med omtrent 18 dager i gjennomsnitt. De mest markante temperaturstigningene ble registrert i Midt og Nord regionene, med årlige temperaturøkninger på opptil 3°C. Nedbørsmønstre har vist en svak økning i Sør og Midt, mens det var liten endring i Nord.

I de nordlige feltene hadde juni-temperaturene den sterkeste korrelasjonen med grunnflatetilvekst (BAI), noe som peker på temperaturbegrensninger for radiell vekst ved disse breddegradene. I motsetning viste de sørlige feltene større følsomhet for juli-nedbør, noe som indikerer en høyere hydrologisk sensitivitet. BAI-analyser indikerer at veksten har stabilisert seg eller økt i nord, mens det har vært en betydelig vekstreduksjon i sør siden 2010.

Samlet sett bekrefter resultatene at veksten i de nordlige områdene primært er begrenset av temperatur, mens de sørlige områdene er mer avhengige av nedbør. Dette bidrar til en bedre forståelse for hvor grensene mellom temperatur- og nedbørsbegrensninger for vekst ligger, under økende temperaturer. Noe som er viktig for å utvikle stedstilpassede skogforvaltningsstrategier i møte med klimaendringer. Fremtidig forskning bør ta en mer helhetlig tilnærming ved å inkludere mer data om skogforhold, utvide til flere felt og treslag for å bedre vår forståelse av klimapåvirkningen på vekst og helse i boreale barskogene.

Contents

1. Introduction

In the shadow of climate change, Norway's expansive spruce (*Picea abies*) forests face an uncertain future. The devastating effects of summer droughts and subsequent bark beetle (*Scolytinae*) attacks in central Europe (Gohli et al., 2024; Karpova et al., 2024; Hlasny et al., 2021) serve as a cautionary tale. A tale that once seemed distant, until Norway's forests succumbed to similar pressures during the 2018 drought (Gohli et al., 2024; Skaland et al., 2019). This event led to substantial drought stress and local bark beetle outbreaks and later raised critical questions about forest management practices and species selection under changing climate conditions.

Traditionally, Norway spruce has been favoured over other species like the, more drought-resistant Scots pine (*Pinus sylvestris*) for forest management practices, due to its higher economic returns and "resilience" to browsing by moose (*Alces alces*). However, this preference comes at a potential ecological cost. Planting spruce on soils typically dominated by pine may amplify the effects of drought, leading to increased vulnerability and subsequently potentially higher mortality rates. These risks are intensified by the impacts of drought, by reducing general forest health and increasing the tree's susceptibility to biotic stressors like insects and pathogens (Netherer et al., 2024; Bentz et al., 2010).

As average temperatures continue to rise, so do predictions for precipitation patterns (Kausrud et al., 2022). An increase in precipitation, especially during spring, contrasts with expectations of more pronounced droughts and heatwaves during the growing season, a paradox highlighted by Hanssen-Bauer et al. (2015). They noted a trend toward longer periods of low river flow in eastern Norway. This trend is attributed to higher winter temperatures, resulting in fewer days with snow cover and earlier snowmelt, which in return leads to potentially lower soil moisture levels, despite higher precipitation levels (Hanssen-Bauer et al., 2015). They further indicate that the thermal growing season in Norway has extended by as much as 2-3 weeks over the past few decades, primarily due to rising spring and autumn temperatures (Hanssen-Bauer et al., 2015). However, this prolongation is accompanied by increasing risks of droughts and shifts in precipitation patterns, especially in eastern Norway, where earlier snowmelt due to higher spring temperatures has reduced soil moisture levels despite higher spring precipitation (Kausrud et al., 2022). Thus, this presents a new set of challenges for spruce trees, which could potentially benefit from increased precipitation and longer growing seasons, but on the other hand, are also known to struggle with drought conditions (Kausrud et al., 2022). Understanding their responses to environmental stressors and different climatic conditions is, therefore, crucial.

Studying the effects of climate change on tree growth is challenging because trees grow slowly, and climate is expected to change significantly over a single tree generation (Linder et al., 2010). Moreover, it is nearly impossible to conduct controlled experiments on mature trees, and greenhouse studies on saplings do not provide a complete picture, as trees in different life stages are expected to react differently to environmental stress (Basler & Körner, 2012).

Natural gradients, such as latitude and elevation, offer valuable insights into climate effects on forest ecosystems. Such “place-for-time” approaches are useful “natural laboratories” for investigating the significance of climatic variations on forest trees. By comparing Norway spruce growth across different sites with varying temperatures and precipitation along a north-south gradient, we can better understand how radial growth may be impacted by climate change (Lyu et al., 2017; Franne et al., 2013).

Dendrochronological analyses, using tree-ring data to assess growth patterns, have proven crucial in studying climate change impacts on forests. By analyzing growth variations over time, dendrochronology offers insights into past climatic conditions and tree responses (Fritts, 1976). Previous studies indicate that Norway spruce growth is significantly influenced by temperature and precipitation, with both climatic factors playing a more crucial role in specific parts of the growing season. Mäkinen et al. (2002) and Andreassen et al. (2006) found that the summer climate significantly affects spruce growth across latitudinal gradients. Northern sites showed stronger correlations with temperature, while southern sites were more influenced by precipitation. Čermák et al. (2019) also observed significant positive correlations between spruce growth and summer temperatures in Norway, but with regional variations in correlation strength. Lie et al. (2023) also highlighted that June precipitation significantly influences Norway spruce growth in south-central Norway.

Climate change is altering the temperature and precipitation patterns, directly impacting the growth and health of Norway's forests. Improving our insights into how spruce growth is influenced by these variations will help forest managers make better-informed decisions. Identifying which climatic factors impact growth the most, and where, by studying the impacts along gradients in Norway will be vital for improving our knowledge and taking measures to mitigate risks both for protecting economic interests and sustainable forest ecosystems.

To address these challenges, this study employs dendrochronological analyses of wood cores to assess the radial growth of spruce trees along a north-south gradient in south-eastern Norway. Through this approach, the aim was to draw comparisons between growth patterns and climatic variables during the growing season, critical for tree development and growth. I hypothesised that 1) mean temperatures and precipitation have significantly increased for all study sites during the life of the study trees, leading to a prolonged growing season and earlier snowmelt. Moreover, that these temperature and growing season length changes are more pronounced in the northern than in the southern part of the gradient. Further, I predicted that 2) Norway spruce growth is limited primarily by precipitation and temperature in June, and 3) that there are differences in responses to climatic variables across the gradient, with northern plots showing stronger correlations between radial growth and temperature and southern plots being more influenced by precipitation levels.

2. Materials and Method

2.1 Study area

The study encompasses ten forest sites along a north-south gradient, covering approximately 325 kilometers from Stor-Elvdal municipality in Rendalen (north) to Aremark municipality (south). These sites fall within the boreal and southern boreal vegetation zones as classified by Moen (1999). The selected locations are situated predominantly inland across Østfold, Akershus, and Innlandet counties (Figure 1), and they reflect a broad range of environmental conditions typical of the southern boreal forest zone. Due to their considerable distance from the coast, these sites typically experience a continental climate, characterized by relatively warm summers and cold winters. However, the Våler and Aremark sites are exceptions, as their relatively close proximity to the Oslofjord subjects them to a more coastal climate with milder winters.

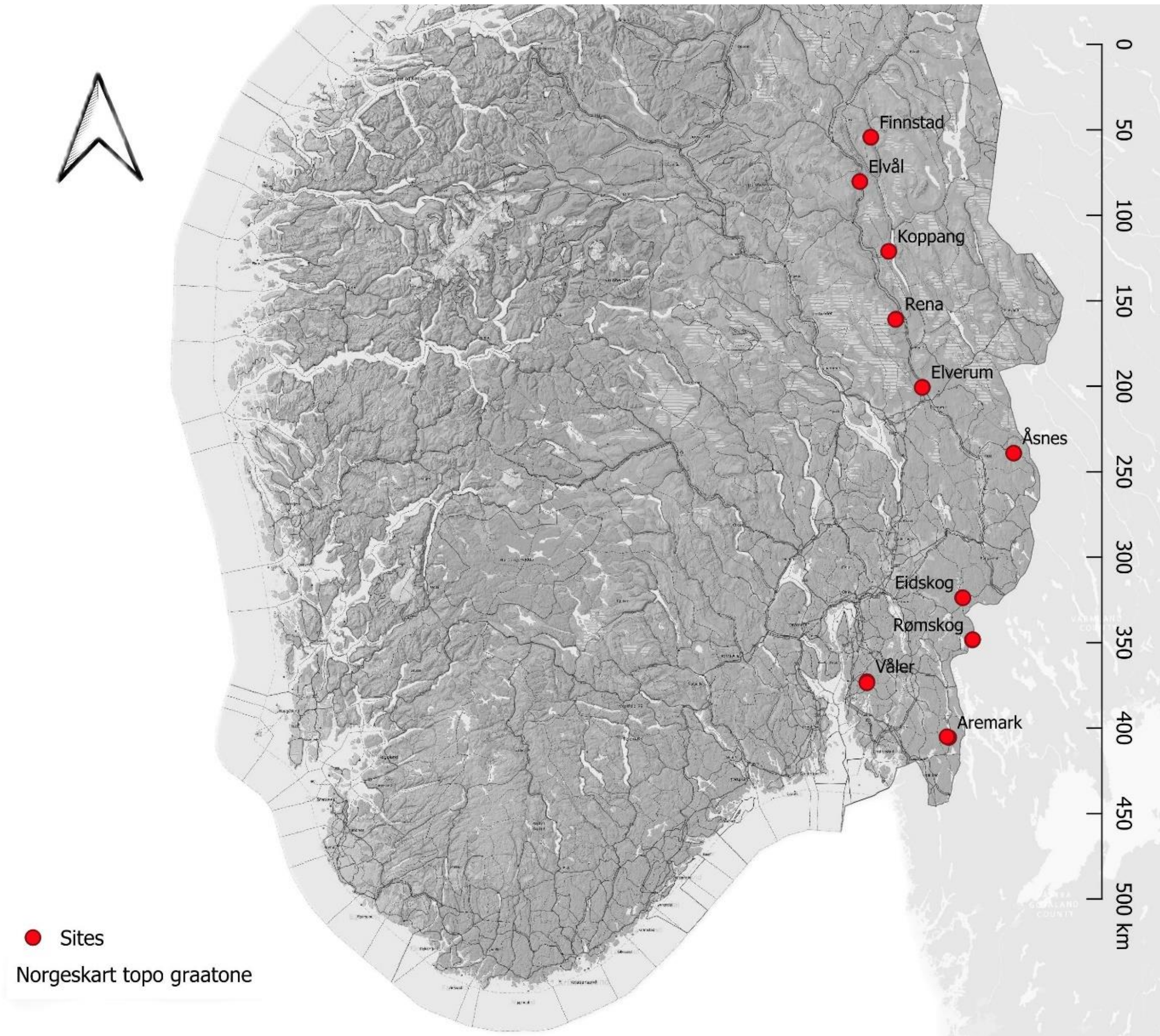

Figure 1. Overview of the geographical location of the experimental sites included in this study. Red dots indicate site location, with their respective names.

The forests in this region predominantly consist of mixed and monospecific coniferous types, with Norway spruce and Scots pine as the most dominant species. There is additionally a significant presence of birch (*Betula spp.*), contributing to the overall forest composition. From south to north, the forests transition from more mixed deciduous/coniferous to predominantly coniferous.

Initiated in the summer of 2022, the experimental setup involves one plot at each site. Each plot measures a circular area of 900m^2 and is strategically located in the middle of forest stands that exceed a minimum size of 0.5 hectares to ensure stable environmental conditions and minimize edge effects. The plots have not been subjected to commercial thinning, ditching, or fertilization and are found in even-aged monocultures, all planted following a clearcut. The forest stands are dominated by Norway spruce, but most plots also have several naturally regenerated Scots pine. The targeted age for the stands was approximately 40 years, with a variation of ±5 years. For plots located on slopes, care was taken to ensure a homogenous slope throughout the plot.

Soil diversity across the sites is notable, ranging from generally more fertile and less rocky podzols and brown soils to more rocky and well-drained podzols.

In setting up the experimental plots, efforts were made to select sites with minimal altitudinal differences to focus on the effects of the north-south climatic gradient, despite the general increase in elevation as one moves further inland (north).

Table 1. Plot information for all sites. Including Plot ID, site names, plot coordinates, site elevation above sea level (masl), mean age from measured cores at breast height, yearly mean temperature and precipitation sum for 1991-2020 and mean diameter at breast height (DBH) for cored trees.

Plot ID	Site	Latitude	Longditude	Elevation	Mean age at breast height	Yearly mean temperature 1991 - 2020	Yearly precipitation 1991 - 2020	Mean DBH cored trees
				masl	years	°C	mm	mm
1	**Aremark**	59.229	11.669	142	34	6.3	1002	220
7	**Våler**	59.516	10.874	82	30	6.5	1040	185
3	**Rømskog**	59.714	11.917	266	32	4.7	936	220
5	**Eidskog**	59.924	11.828	284	38	4.5	926	216
9	**Åsnes**	60.624	12.357	323	37	4.0	850	183
11	**Elverum**	60.948	11.47	270	29	3.7	1030	190
13	**Rena**	61.274	11.222	525	28	2.2	1046	246
15	**Koppang**	61.593	11.163	642	23	1.7	616	189
17	**Elvål**	61.92	10.889	483	49	1.8	560	195
19	**Finnstad**	62.123	11.006	479	22	2.1	578	168

2.2 Data collection

2.2.1 Tree-ring data

During the summer months of June and July 2023, tree rings were sampled by coring selected trees at breast height, which is standardized at 130cm above the stump. A standard 5mm diameter increment borer (Haglöf AB., Sweden) attached to a battery-powered hand-drill was used for extracting cores from the trees. The coring process adhered to standardized protocol to ensure consistency. Specifically, one core was taken per tree, targeted on the north side of the trunk, perpendicular to the slope. For instances where coring perpendicular to the slope at breast height would not yield a satisfactory core, such as in the presence of a branch, adjustments were made to take the sample more on the uphill side of the tree. This adjustment was aimed at maintaining a standardized coring method while minimizing the potential for including compression wood in the core samples.

In each plot, a minimum of six dominant spruce trees were carefully selected for coring. Additionally, six co-dominant trees equipped with dendrometers were included in the sampling process. The dendrometer-fitted trees were chosen for their representation of healthy, average specimens centrally located within each plot. Their inclusion in a separate study influenced the overall selection process. As a result, my dataset of cores consists of half the samples from dominant trees and half from co-dominant trees.

To determine the dominant trees, diameter at breast height (DBH) was utilized, selecting the largest trees as the most dominant. The selection process was streamlined by employing a list organized by descending DBH. During the quality check, emphasis was placed on ensuring the health of the trees. Criteria for selection included healthy appearance, straight growth, and absence of deformities such as top breaks, split tops, or crooked stems. Trees with visible wounds, irregular or oval stems, or bulging rootstocks were excluded.

In certain plots, not all the dominant trees met the selection standards. In such cases, dominant trees with slight irregularities, such as an oval stem shape were cored, but higher on the trunk where the shape was round. This issue was more prevalent among the dendrometer trees. This was the case for one dominant spruce in plot 7 and one dendrometer spruce in plots 3, 5, 11 and 14, as such they were excluded from mean DBH calculation. In the Elvål site, two dominant spruce trees were significantly older than the other cored trees, by approximately 20 years. These outliers were therefore not included in the mean age and mean DBH calculations.

Moreover, to avoid any potential edge or gap effects, trees on the borders of the plots were not sampled. This ensured that each selected tree was well-integrated within the forest stand, surrounded by at least one "line" of neighboring trees, thereby ensuring that selected trees represented the most robust and healthy individuals within each plot.

Post-collection, the cores were placed and stored in labeled plastic tubes with lids. After all cores were collected from a plot, a 50/50 ethanol/glycerol mixture was added to the plastic tubes to prevent shrinking or deformation. At the end of each sampling day, the cores were placed in a cooler for preservation until they were all shipped to CzechGlobe in Brno. Overall, a minimum of 12 cores were sampled for each plot, resulting in a final number of 125 collected spruce cores from the studied plots.

2.2.2 Climate data

The climatic data utilized were sourced from the seNorge2 dataset provided by the Norwegian Meteorological Institute (MET) (Lussana et al., 2018). This dataset offers high-resolution, daily mean climatic data, including total precipitation, mean temperature, maximum temperature, minimum temperature, and snow depth. The dataset is gridded with a 1 km spatial resolution, encompassing the Norwegian mainland. It spans the years from 1957 to the present, with daily updates available for recent years (Lussana et al., 2018). For the purpose of my analysis, I focused on the period from 1960 to 2022. The earlier years, particularly 1957, were excluded due to missing climatic values for some of the sites. Additionally, data for 2023 was omitted to ensure consistency with the dendrochronological record, as the growth ring for 2023 was incomplete.

The seNorge2 dataset is constructed using a combination of in situ observations from the Norwegian Climate Database and the European Climate Assessment Dataset (ECA&D). The observations are interpolated using a statistical method based on optimal interpolation (OI) and successive-correction schemes (Lussana et al., 2018). This method ensures the representation of local precipitation features at spatial scales of a few kilometers, dependent on the density of the observation network (Lussana et al., 2018).

2.3 Data processing

2.3.1 Sample preparation

The processing and measurement of the tree-ring cores began with the samples being sent to CzechGlobe in Brno. In collaboration with Mendel University, the cores were prepared for measuring using a sliding microtome table. This procedure involved carefully shaving micrometres off each sample to create a flat surface suitable for precise measurement of tree ring widths. Once prepared, the cores were put back in their original plastic containers containing the 50/50 ethanol/glycerol mixture.

After the initial preparation, the cores were placed in wooden slots to partially dry. The partially dried samples were then scanned using a high-resolution digital scanner. The digital images obtained were analysed using the Coorecorder software to measure tree ring widths accurately (Larsson, 2013).

2.3.2 Crossdating

Following the scanning and measuring process, all transect cores were cross-dated using C-dendro software (Larsson, 2013). This step involves comparing the measured tree ring series from individual trees within a plot to see if their growth pattern align, indicating similar trends in growth.

Problematic cores and plots that generally did not cross-date well were noted and subsequently remeasured later. Remeasurement involved the use of a LINTAB tree-ring measurement station (Rinntech e.K., Germany) and a Leica microscope (Leica Microsystems GmbH., Germany), capable of measuring with an accuracy of 0.01 millimetres. After the remeasuring of specific cores and plots, all cores were re-cross-dated using the Past4 software (SCIEM - Scientific Engineering and Manufacturing).

During the cross-dating process, any core that would not cross-date with the other cores from the plot was excluded from the final analysis. The purpose of this was to include a robust dataset with well-cross-dated cores from each plot. Trees were still forming their 2023 ring at the time of collection, as such the last incomplete ring was not measured.

To check for any discrepancies in the measurements, before statistical analysis and conversion of the tree ring data, xDaterR interactive web-based application was used (Bunn et al., 2023). This was done to make sure the measurements were well cross-dated and that especially the last ring (2022) was the same for all samples. After the final cross-dating I was left with an average of 9 out of 12 trees per site.

2.4 Statistical analysis

2.4.1 Climatic data

The daily climatic data (Lussana et al., 2018) were aggregated into monthly and yearly resolutions for the dendrochronological analyses. Annual data were visualized using scatter plots and analysed with linear regression models to calculate the average annual changes in temperature and precipitation from 1960 to 2022. The same methodology was applied to determine changes in the snowmelt date, defined as the last day with snow cover rather than the first day without snow.

Thermal growing season calculation and methods

For calculating the thermal growing season, the “vegperiod” package in R (Nuske, 2022; R Core Team, 2023) was used. Two different methods were used and compared to calculate the start of the growing season and three methods were used and compared to determine the end of the potential growing season. By employing and comparing multiple methods the aim was to avoid biases and gain a more comprehensive understanding of the change in thermal growing season.

StdMeteo: The StdMeteo method calculates the start and end of the growing season based on a temperature threshold. To determine the onset of the growing season, this method identifies the first occurrence of at least five consecutive days where the daily average air temperature is above 5°C. Similarly, the end of the growing season is marked by at least five consecutive days with daily average temperatures falling below 5°C. This approach assumes that a sustained period of five days is significant enough to indicate a reliable change in season (ETCCDI, 2009; Frich et al., 2002; Zhang et al., 2011). This generally leads to the onset of growing season to occur quite early in the spring, and a quite late vegetation end in the fall, as the approach awaits sustained low daily mean temperatures.

Menzel: The Menzel method calculates the start of the growing season by assessing chill days from the previous November and December. The method then tracks the accumulation of heat beginning in February, calculating a “HeatSum” of daily mean temperatures that exceed a critical base temperature from a species-specific regression formula. The growing season for each species starts when this HeatSum surpasses a predetermined critical threshold (Menzel, 1997). For this specific study both the “Picea Abies (noerdl)” Norway spruce, Northern) and “Picea Abies (frueh)” (Norway spruce early) regression formulas were used.

VonWilpert: The vonWilpert method employs a 7-day moving average of daily temperatures, requiring at least five consecutive days below 10°C to signal the end of the season. If temperatures rise above 10°C for more than five days subsequently, the growing period resumes. Additionally, the method sets the final day of the season as day 279, based on a short-day criterion (von Wilpert, 1990). This method was first developed for Norway spruce in the “Black forest” in Germany, but has later been applied for multiple species and for other regions.

NuskeAlbert: Similarly to the method above, the NuskeAlbert method relies on a 7-day moving average of daily mean temperatures, marking the end of the season when there are five consecutive days with temperatures below 5°C, starting the search from July 1st. Additionally, regardless of temperature, the method designates October 5th as the ultimate end of the vegetation period based on a short-day criterion (Walter & Linderholm, 2006).

2.4.2 Tree ring data

The tree-ring series were converted from annual tree ring widths (TRW) to basal area increment (BAI) using the bai.out function from the dplR package, which converts ring width measurements into area measurements (Bunn et al., 2023). The R function calculates bai by considering the measured DBH and the width of each ring, going from the bark to the pith.

BAI series were then detrended using the smoothing spline method. This method removes long-term trends related to age and size as well as other disturbances, emphasizing the common climate-related variance within sites (Fritts, 1976). The standard smoothing spline method from the dplR package in R was used (Bunn et al., 2023; R Core Team, 2023). Statistical parameters for quality assessment of the data such as First-order autocorrelation (Ar1) and Mean sensitivity (MS) were derived from the raw BAI series. In contrast, mean interseries correlation (Rbar) and expressed population signal (EPS) were calculated from the detrended BAI series (Table 2).

Subsequently, the detrended residual chronologies for each plot were analyzed to uncover correlations between annual BAI and climatic variables of mean temperature and precipitation from the previous April to the current September, using the "treeclim" package and the "dcc" function in R (Zhang & Biondi, 2022). This analysis, covering the period from 1995-2022, helps to understand how tree growth responds to climatic factors, especially summer temperatures and precipitation.

2.4.3 Quality assessment

Tree-ring chronologies were assessed using different descriptive statistical measures to evaluate the signal quality and the potential for climate reconstruction and correlation.

First-order autocorrelation (Ar1) was computed from raw BAI to evaluate the persistence of growth patterns, which helps in understanding the influence of the preceding year's growth on subsequent years (Fritts, 1976; Speer, 2010).

Further, Mean Sensitivity (MS), which quantifies the relative change in tree-ring widths from one year to the next, was evaluated to assess each tree's responsiveness to inter-annual environmental fluctuations. A higher mean sensitivity suggests a pronounced variability in growth, characteristic of trees in environments where growth dynamics are significantly influenced by annual climatic variations (Bunn et al., 2013).

Additionally, the mean inter-series correlation (Rbar) was calculated to assess the common signal among the tree-ring width series. This statistic measures the coherence of growth patterns across multiple trees within a site, where higher values indicate a stronger common signal, potentially related to regional climatic influences. While there is no specific “ideal” Rbar value, generally the higher the Rbar value the better. Higher values indicate a stronger common signal, reflecting more consistent climatic influences across the sampled trees (Bunn et al., 2023).

Expressed Population Signal (EPS) was derived to estimate how well the sample chronology represents the population-level variability. EPS is a key metric in dendrochronology, indicating the signal-to-noise ratio in a finite chronology and its ability to approximate the theoretical population chronology. Typically, an EPS value close to 1, or above a 0.85 threshold suggests a strong common signal and is preferred for climate reconstructions (Buras, 2017; Wigley et al., 1984).

For the tree-ring series in this study, statistical computations were conducted using the dplR package in R, which is designed specifically for dendrochronological analysis (Bunn et al., 2023). Notably, due to the young ages of the trees in plots 15 and 17, Rbar and EPS values are not presented, as the short length of the tree-ring series could lead to less reliable estimates of these statistics. The established threshold of 0.85 for EPS, commonly used in dendrochronological studies, serves as a reference point for evaluating the suitability of the chronology for reconstructing climatic variables, though it should not be considered a definitive cutoff.

Table 2. Quality assessment of the developed BAI chronologies for plots with site location, number of sampled trees (N), mean length of series, time span, first order autocorrelation (Ar1), mean sensitivity (MS), mean inter-series correlation (Rbar) and expressed population signal (EPS). Plots 15, and 17 don't display values Rbar and EPS values because of the young ages of the stands.

Plot ID	Site	N	Mean age	Time span	Ar1	MS	Rbar	EPS
1	**Aremark**	9	34	1986-2022	0.82	0.23	0.47	0.89
3	**Rømskog**	9	31	1989-2022	0.76	0.26	0.55	0.91
5	**Eidskog**	9	38	1979-2022	0.78	0.22	0.36	0.84
7	**Våler**	7	30	1992-2022	0.75	0.30	0.54	0.89
9	**Åsnes**	11	37	1983-2022	0.68	0.26	0.38	0.87
11	**Elverum**	8	31	1990-2022	0.75	0.26	0.40	0.82
13	**Rena**	8	28	1992-2022	0.69	0.24	0.54	0.70
15	**Koppang**	12	24	1996-2022	0.65	0.30	-	-
17	**Elvål**	9	53	1946-2022	0.78	0.22	0.34	0.82
19	**Finnstad**	8	22	1998-2022	0.72	0.30	-	-

2.5 Dividing geographical regions

The sites were divided into three geographical regions to present the climate-growth correlations in a clear and structured manner. The classification was based on results from the “dcc” function in addition to location and climatic characteristics, particularly focusing on temperature and precipitation patterns (Table 3).

Table 3. Overview of the division of the three geographical regions, South, Mid and North.

Region	Sites
South	Aremark, Våler, Rømskog, Eidskog
Mid	Åsnes, Elverum
North	Rena, Koppang, Elvål, Finnstad

The Mid region presented a classification challenge, as the Rena site displayed precipitation patterns similar to the Mid region but temperature patterns comparable to the North region (Table 1). Despite these similarities in precipitation, the decision was made to classify the Rena site under the North region due to the following reasons:

- Summer precipitation (May-Aug) did not deviate as significantly from the northern sites, even though winter precipitation did.
- The Rena site is situated approximately 250 meters above the valley floor. This elevation impacts temperature, aligning the site more closely with the Sites in the North region.
-

3. Results

3.1 Climate

Mean temperatures have increased significantly from 1960 to 2022 across all sites, with an average temperature rise of 2.7°C across sites (Figure 2A). The most notable increase in mean temperatures has occurred in the Mid and North regions, with the Åsnes site showing an annual temperature increase of 3.25°C for the respective period (Table 4). The increase in temperatures has been accompanied by a more modest change in precipitation sums, with some sites observing a substantial increase in precipitation, while others observe little to no change (Figure 2B). This variability in precipitation across different regions highlights the different interactions between temperature increases and moisture availability, which could have significant implications for tree growth.

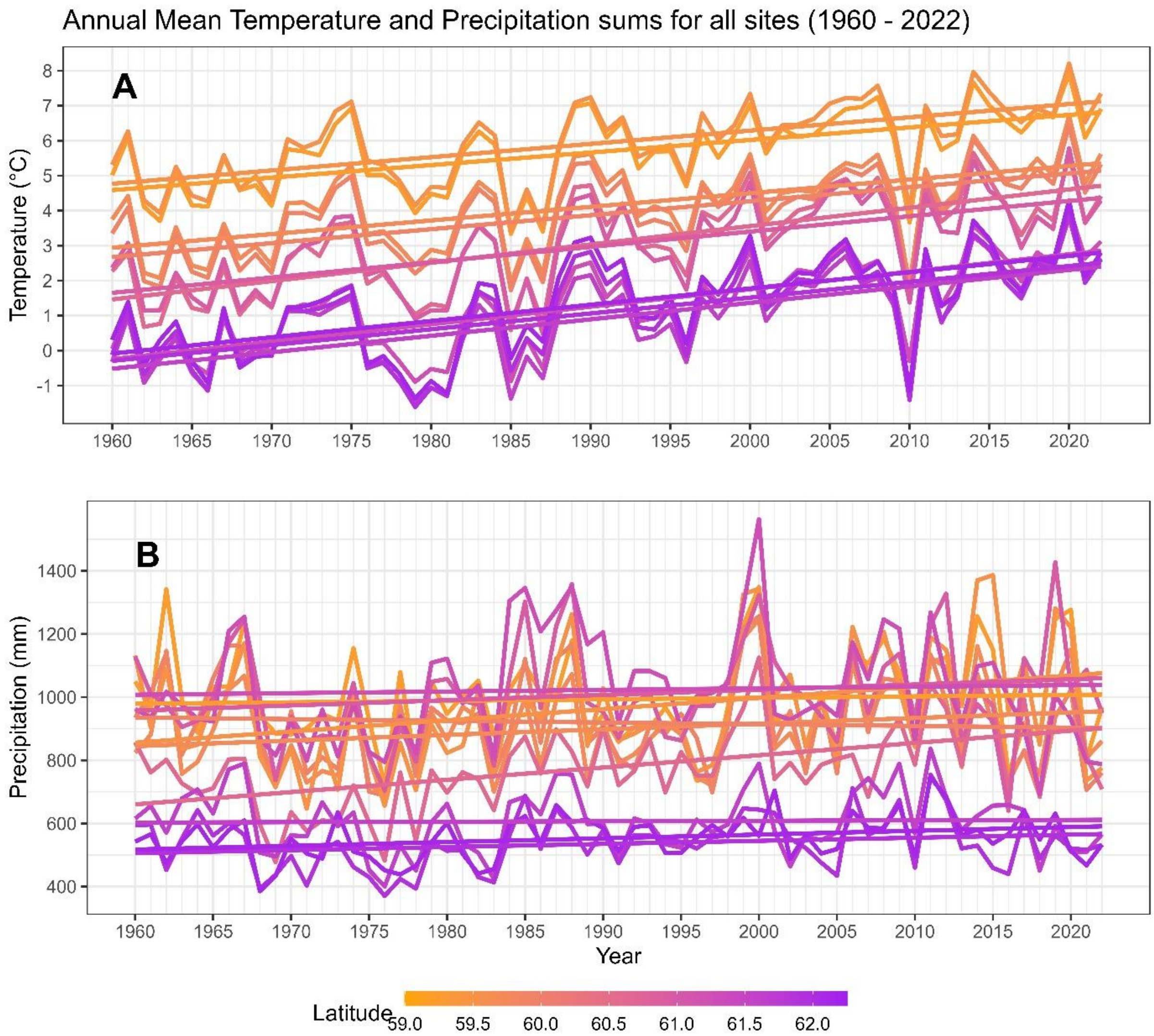

Figure 2. Annual mean temperatures (A) and precipitation sums (B) for all study sites from 1960 to 2022. Sites are color-coded from orange (southern) to purple (northern) according to latitude. Regression lines indicate trends in temperature and precipitation over the studied period.

Further, my analysis revealed a significant extension of the thermal growing season (TGS) across all studied sites, averaging approximately 18 days across methods, varying from 10 to 27 days depending on the site and method used for calculation. Changes were particularly notable using the StdMeteo and the combined Menzel/VonWilpert method (Table 4). While all three methods indicate significant prolongation of the TGS, the Menzel/VonWilpert methods generally exhibit a higher level of statistical significance ($p < 0.001$), especially in the northern regions where the TGS extension is most pronounced. The TGS prolongation was more pronounced in some sites, in particular, Våler using the StdMeteo method (Table 4).

Furthermore, the advancement in snowmelt timing aligns with the changes observed in TGS. Snowmelt is occurring increasingly earlier, marking a significant shift in hydrological cycles, and potentially affecting water availability in these regions. Notably, sites like Eidskog and Elverum have witnessed the last snow day occurring approximately 23 and 28 days earlier in 2022 compared to 1960, respectively. While most values show significance, the rate of change (r-value) varies between sites, suggesting differences across locations, with the northernmost sites showing little change.

While these changes are statistically significant across all sites, the rate of change in temperature, precipitation, and TGS varies, suggesting that local factors and microclimates play a crucial role in modulating these responses. These variations underscore the complexity of climate impacts on different geographical locations.

*Table 4. Summary of climatic changes and thermal growing season (TGS) shifts for each study site from 1960 to 2022. Displaying the shift in mean annual temperatures and precipitation sums. Additionally, the advancement of the TGS in days shown for three different calculation methods, and an advancement in the snow melt date. Asterisks indicate significance and are marked as follows: * for p < 0.05, ** for p < 0.005, and *** for p < 0.001. Results are based on linear regression analysis of the 1960-2022 daily climatic data.*

Change from 1960-2022

				TGS change			
Region	**Site**	**Yearly Mean Temperature**	**Yearly Precipitation**	**StdMeteo**	**Menzel/ VonWilpert**	**StdMeteo/ NuskeAlbert**	**Snow melt**
		°C	**mm**	**days**	**days**	**days**	**days**
South	**Aremark**	2.22 ***	30	18 *	14 **	19 ***	-20 ***
	Våler	2.35 ***	220 **	24 **	15 ***	17 ***	-12
	Rømskog	2.41 ***	112	14 *	18 ***	12 **	-20 ***
	Eidskog	2.47 ***	-33	14 *	20 ***	10 *	-23 ***
Mid	**Åsnes**	3.25 ***	241 ***	24 ***	22 ***	16 ***	-22 ***
	Elverum	2.71 ***	103	17 **	22 ***	11 **	-28 ***
North	**Rena**	3.10 ***	32	20 **	26 ***	20 ***	-13 **
	Koppang	2.92 ***	9	19 **	27 ***	19 **	-14 **
	Elvål	2.80 ***	61	18 **	26 ***	18 **	-8
	Finstad	2.88 ***	74 *	16 **	23 ***	16 **	-6

When the data is segmented into geographical regions by latitude, distinct variations in climate patterns for May through July are revealed (Figure 3), showing a clear warming trend for mean temperatures during the early summer months (Figure 3A). This trend is statistically significant across all regions, but with the Mid and North regions exhibiting the most pronounced warming.

For precipitation (Figure 3B), changes are less uniform, reflecting greater variability and a less consistent trend in early summer rainfall across the decades. While the South and Mid regions show a mild increase in precipitation with some statistical significance (Table 4), the North region experiences minimal, non-significant changes. This suggests that while temperature trends show a clear warming pattern, precipitation responses are more varied and influenced by regional factors.

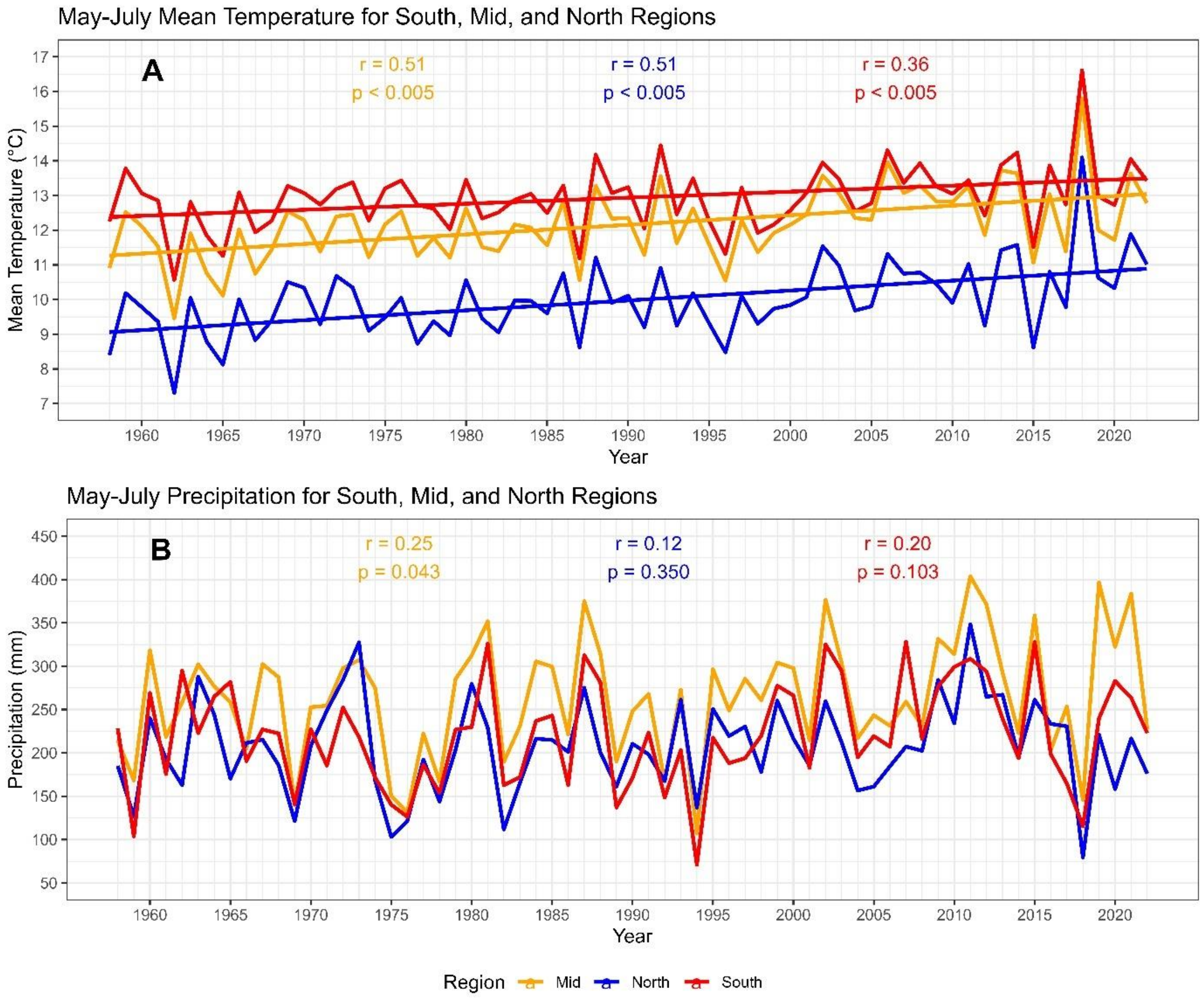

Figure 3. May-July mean temperature (A) and precipitation sum (B) for the three regions South (red), Mid (orange), and North (blue) 1960 and 2022. Statistical values are based on linear regression models and highlight how temperature and precipitation have changed over time for the early summer.

3.2 Basal Area Increments (BAI)

Analysis of raw Basal Area Increments (BAI) across the southern plots shows a notable peak in growth around 2010, followed by a pronounced decline through 2019, following the severe drought period from May to July 2018 (Figure 4). This decline is marked by significant reductions in BAI, particularly emphasized by pointer years identified in 2006, 2015, and 2019, where each represents notable climatic impacts followed by recovery phases. In contrast, the northern plots exhibit a divergent pattern, largely absent of significant declines, despite experiencing similar drought conditions (Figure 5). After 2006, northern plots show a trend toward stabilization in BAI, with smaller fluctuations. This suggests region-specific growth responses, possibly due to differences in local climate resilience or other environmental factors. Noteworthy is the stabilization or increase post-2010 in northern regions, contrasting sharply with the southern decline during the same period (Figure 4 and 5).

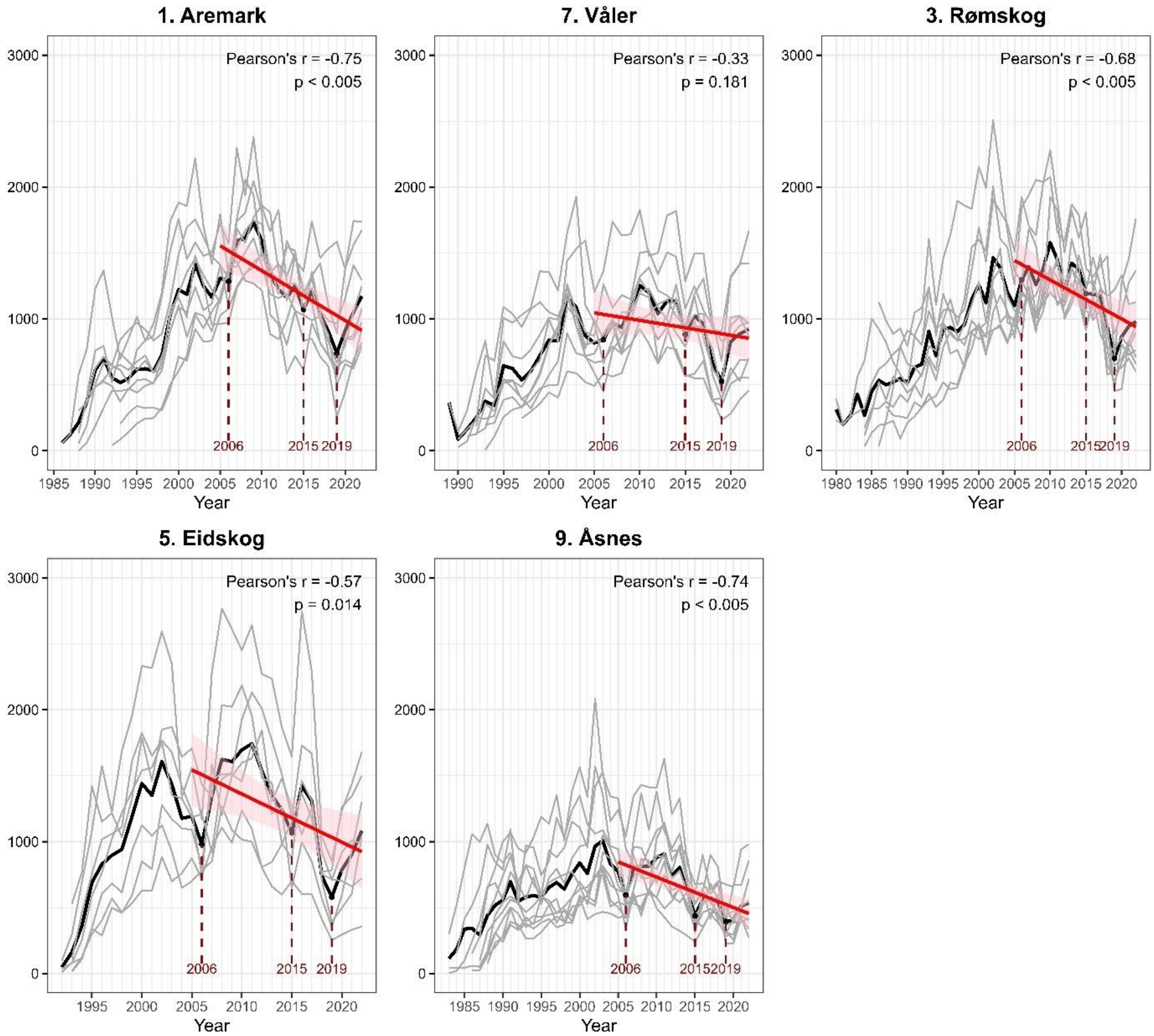

Figure 4. Raw basal area increments (BAI) in mm² for Southern plots over time. Grey lines indicate individual tree samples, while black lines indicate the mean BAI for the respective plot. The Y-axis is consistent across plots, showing BAI values, but the X-axis differs to account for varying ages at breast height. Red line indicates a regression line with 95% confidence interval, with Pearsons-r and p-value for statistical parameters. Pointer years are marked as red stippled lines.

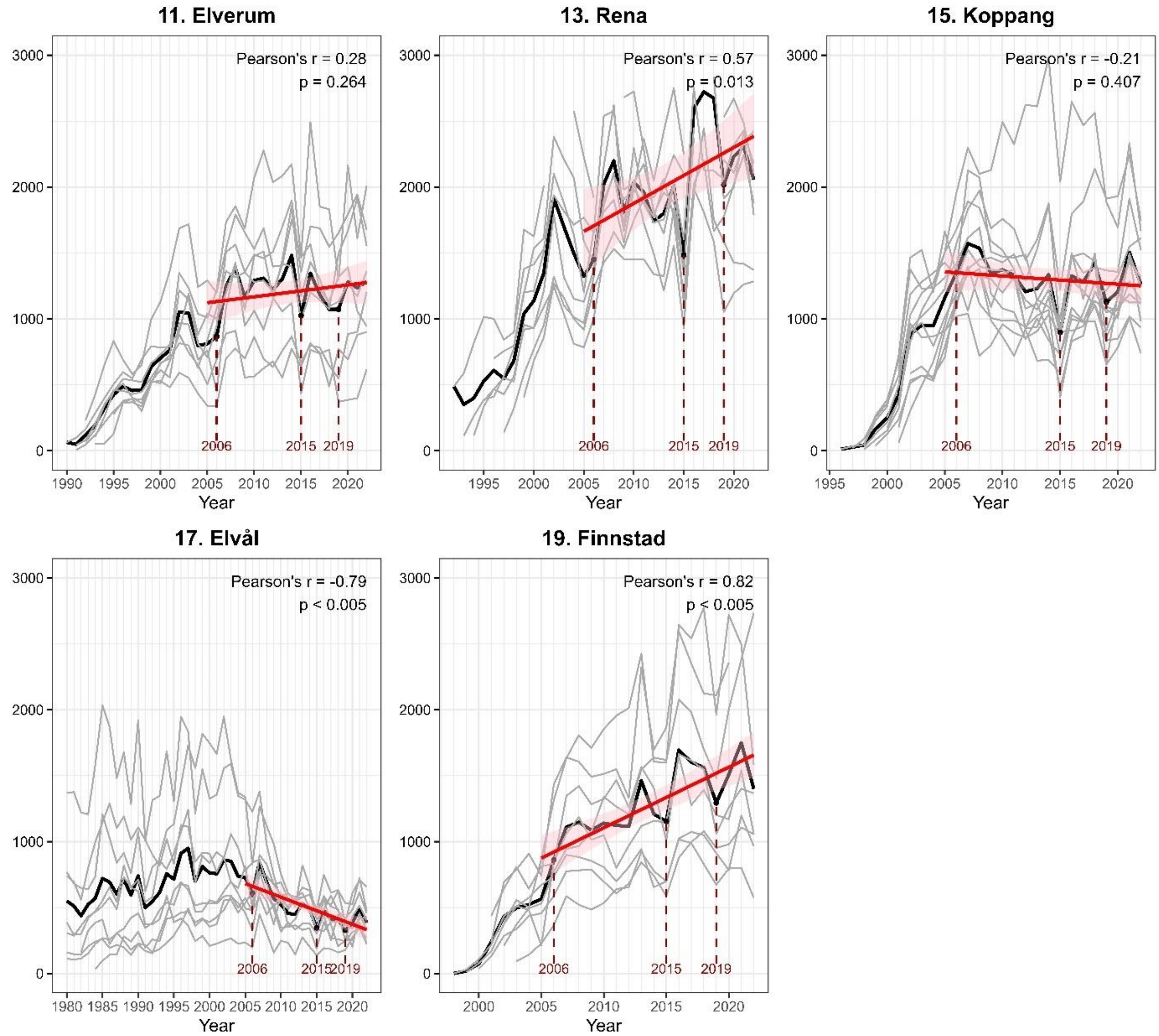

Figure 5. Raw basal area increments (BAI) in mm² for Northern plots over time. Grey lines indicate individual tree samples, while black lines indicate the mean BAI for the respective plot. The Y-axis is consistent across plots, showing BAI values, but the X-axis differs to account for varying ages at breast height. Red line indicates a regression line with 95% confidence interval, with Pearsons-r and p-value for statistical parameters. Pointer years are marked as red stippled lines.

Detrended "spline" chronologies spanning from 2000 to 2022 unveil distinct trends in tree growth across various latitudes (Figure 6). By employing a "spline" detrending method, age and size-related growth trends are effectively removed, allowing for more accurate representations of environmental influences on tree growth. The refined chronologies emphasize the years when adverse climatic conditions most significantly impacted tree growth, providing critical insights into the environmental stressors affecting forest health.

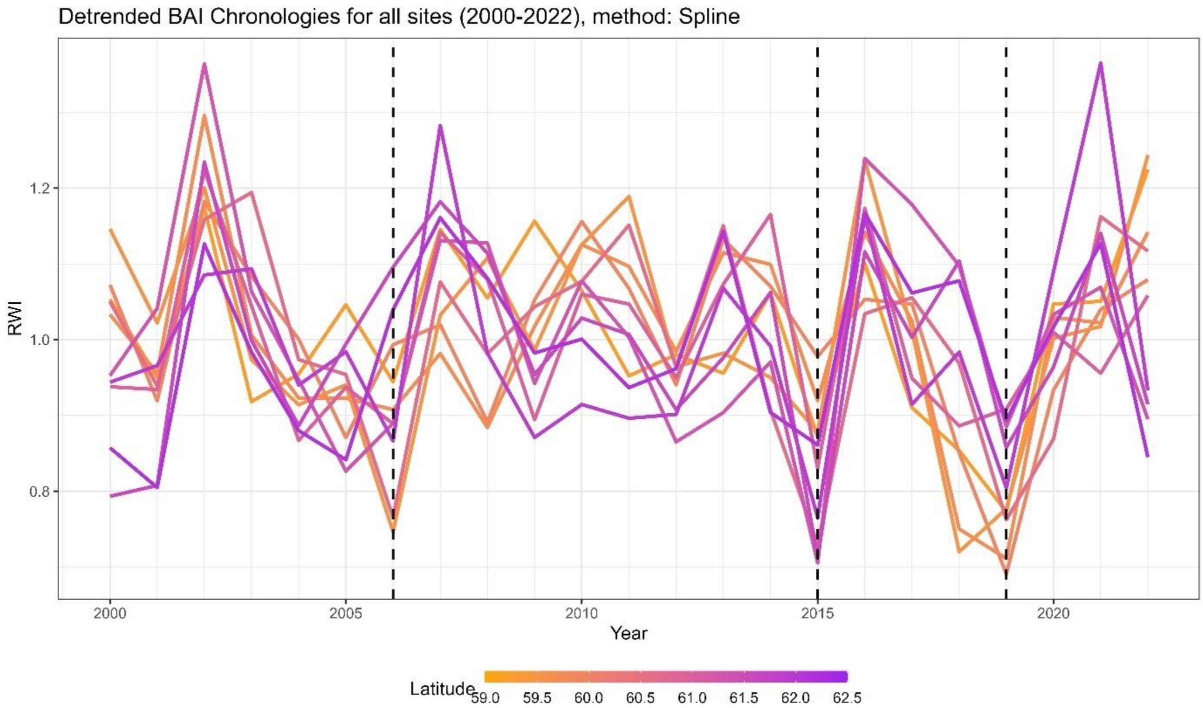

Figure 6. Detrended BAI chronologies from (2000 to 2022), color-coded by latitude to illustrate regional variations in growth patterns. The Y- axis displays the Residual Wood Index (RWI), emphasizing normalized growth rates. Significant dips in growth corresponding to the pointer years – 2006, 2015 and 2019 are marked with stippled lines.

3.3 Climate-Growth correlation

The analysis of climate-growth correlations, based on Basal Area Increment (BAI), reveals distinct regional differences. In the southern region, precipitation is closely correlated with BAI, particularly in July of both the current and previous years, showing significant positive correlations (Figure 7). This pattern highlights the southern region's higher hydrological sensitivity, suggesting that precipitation is a crucial factor in radial growth.

In the Mid region, the correlation data indicate a positive relationship between BAI and precipitation from the previous July, alongside a modest positive correlation with precipitation in June of the current year, reflecting a nuanced influence on growth.

On the other hand, in the northern region, temperature shows a more substantial correlation with BAI. Notably, current June temperatures demonstrate a significant positive correlation with radial growth. This finding underscores the critical role of thermal influences on radial growth in higher latitudes, where temperatures are generally lower, marking a contrast to the more precipitation-driven growth patterns observed in the southern region.

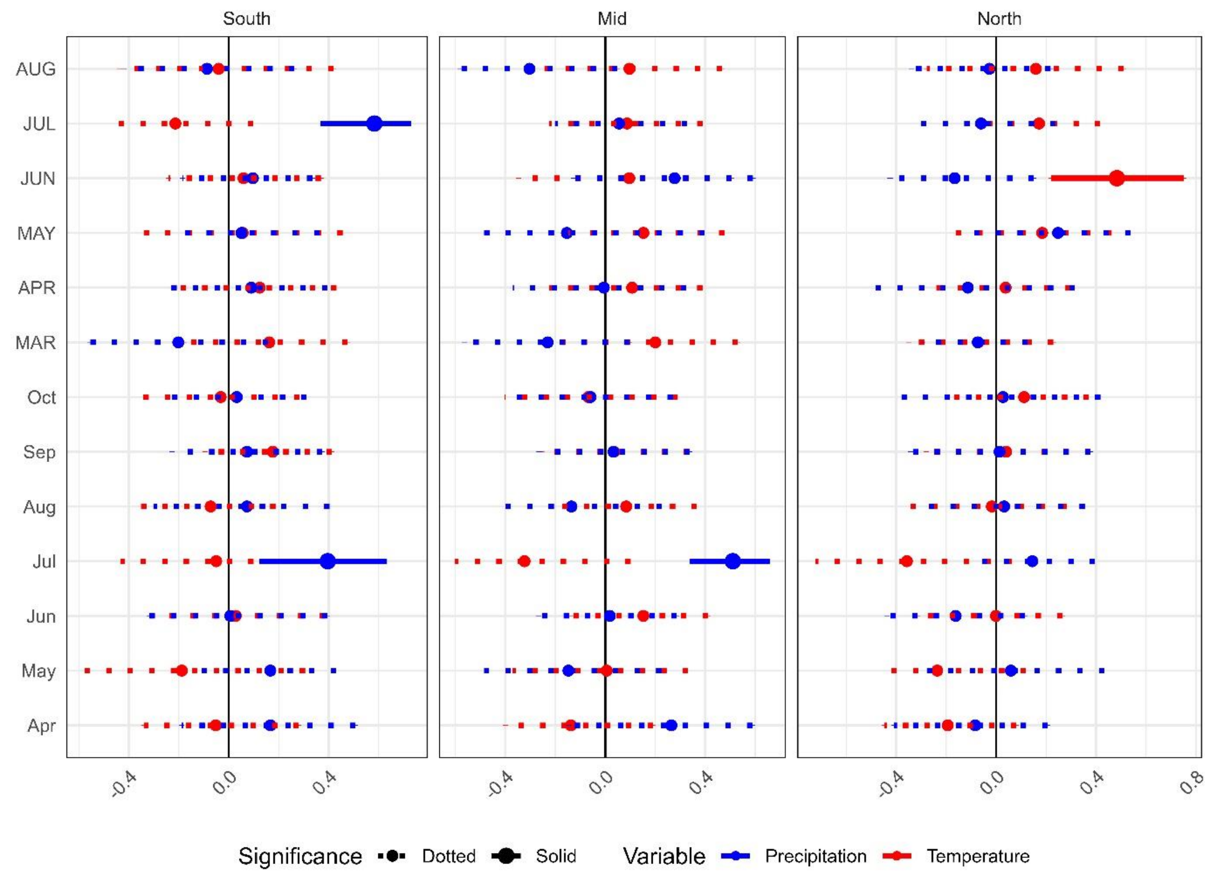

Figure 7. Illustrating the correlation between monthly precipitation (blue) sums and mean temperatures (red) with radial growth for three geographical areas: "South" (plots 1, 7, 3, 5), "Mid" (plots 9 & 11), and North (plots 13, 15, 17, 19). The Y-axis represents the months, with lowercase letters denoting the previous year and the uppercase letters signifying the current year. The X-axis quantifies the correlation coefficients, with stippled lines indicating non-significant correlations and solid lines indicating significant ones. Notably, the distance of the horizontal lines from 0, indicates the strength of the correlation, while the width of the lines is indicative of confidence interval.

4. Discussion

Boreal forests are increasingly threatened by climate change, and Norway spruce is particularly vulnerable to rising temperatures, altered precipitation patterns, and more frequent abiotic and biotic disturbances such as droughts and bark beetle outbreaks (Hartmann et al., 2022; Allen et al., 2010; Hlasny et al., 2021; Netherer & Hammerbacher, 2022). Additionally boreal forests play a crucial role in carbon sequestration, potentially storing more carbon than any other terrestrial biome, emphasising the importance of understanding their response to ongoing climate change (Bradshaw & Warkentin, 2015; Pan et al., 2011). Soil moisture levels, and temperature influence water flux and carbon accumulation in trees and play an important role in radial growth (D'Andrea et al., 2023; Greisbquer et al., 2021). This study used tree rings to explore the growth of Norway spruce across a north-south gradient, providing valuable data to study regional variations in radial growth due to latitudinal differences in climate. The climate-growth correlation analysis revealed distinct regional differences in growth responses, offering insights into the varied climatic sensitivities of Norway spruce across the studied gradient.

As hypothesized, this study found a significant increase in yearly temperatures across all sites, with the most substantial rise occurring in the mid and northern regions, featuring an almost 3°C average temperature increase since 1960. The same trend was also evident for temperatures during specific months (Figure 3B). Additionally, the overall trend of precipitation across the study sites indicated a slight upward shift, consistent with observations of increasing precipitation in Norway during the same period, as reported by Lutz et al. (2024).

Likewise, the Thermal Growing Season (TGS) and the timing of snowmelt have significantly extended across all locations (Table 2), validating the predictions made by Hanssen-Bauer et al. (2015) regarding the impact of rising temperatures on earlier snowmelt and prolongation of TGS. Grundmann et al. (2011) and Čermák et al. (2019) also observed more marked warming trends at higher latitudes, consistent with the higher temperature increase observed in the mid and northern sites, underscoring significant climatic shifts affecting these areas. These findings collectively confirm the first hypothesis, indicating that temperature and growing season have significantly changed during the life of the studied trees and that changes are indeed more pronounced in the northern part of the gradient compared to the southern part.

In examining the specific impacts of climate on Norway spruce growth, I hypothesized that June temperature and precipitation would strongly correlate with growth patterns and that these correlations would vary along the north-south gradient. Indeed, the data collected revealed distinct regional variations in growth responses, providing insights into the varied climatic sensitivities of Norway spruce across the gradient.

Northern sites displayed strong correlations with June temperature, confirming its significant influence on growth. In contrast, southern sites demonstrated the most pronounced correlation with July precipitation. The mid site on the other hand displayed a more nuanced pattern with current June precipitation showing a moderate correlation, and previous July precipitation showing a significant correlation, more like the southern sites. These findings align with other Scandinavian research that underscores June as a critical month influencing growth at various latitudes and altitudes (Andreassen et al., 2006; Mikanen et al., 2002; Lie et al., 2023). Additional studies across Europe support these observations, noting a more substantial impact of temperature on growth at higher latitudes and altitudes, while areas at lower altitudes and southern latitudes are predominantly limited by precipitation (Popa, 2022; Bošelá et al., 2021; Čermák et al., 2019). Moreover, studies by Grundmann et al. (2011), Andreassen et al. (2006) and Čermák et al. 2017 have highlighted the importance of summer precipitation for radial growth, further supporting these observations.

Interestingly, despite many studies emphasizing the critical role of June precipitation, my findings indicate that July precipitation has a more significant impact on growth in southern and mid sites. This is likely due to lower soil moisture levels during this period. My findings suggest that precipitation in July is the most limiting factor, similar to Bošelá et al. (2014), who also found July precipitation critical for growth in lowland sites.

The regional differences in climatic sensitivity are also evident in the raw BAI series. Southern plots show a peak in growth around 2010, followed by a decline through 2019, coinciding with the 2018 drought (Figure 4). In contrast, northern plots exhibited more stable BAI patterns, trending towards stabilization or increase after 2010 (Figure 5). This divergence suggests region-specific factors influencing resilience to drought, potentially linked to tree ages and varying drought impacts during marker years.

Voelker (2011) demonstrated that radial growth rates in trees under 50 years old are more dependent on precipitation due to their shallower rooting depths. This implies that older forests, with deeper-rooted trees, might be more resilient to short-term droughts. However, the southern site trees are generally older, except at the Elvål site, suggesting that other factors are at play.

Furthermore, Bošel’a et al. (2021) found that spruce populations growing at lower elevations and latitudes were more vulnerable to drought, likely due to higher temperatures and subsequently higher evaporation rates. Bošel’a et al. (2021) also noted that, even though lower and higher elevation sites showed slightly different responses to fluctuations in temperature and precipitation, they generally showed a synchronized growth reaction, which is consistent with my data.

Popa (2022) found that BAI at high elevations in the Eastern Carpathians exhibits a strong temperature signal, particularly in early summer. This finding is comparable to the northern plots in my study, where growth is also limited by temperature. High early summer and late spring temperatures positively impact growth in this region. The timing of the 2018 drought (May – July) can explain the varied responses across regions (Skaland et al., 2019). Northern plots, with higher snow cover and later snowmelt, likely maintained higher soil moisture levels, mitigating the impact of the drought, despite equally adverse conditions across regions. Thus, the combination of beneficial temperatures and moister soils resulted in a lesser drought effect in the north.

Though the 2018 year impacted growth differently across the regions, the marker years (Figure 4 & 5) have in common that they occur one year after unfavorable climatic conditions. The 2006 marker year reflects a period from 2004-2006 with below-average precipitation during May-July, particularly affecting the north and mid regions more (Supplementary Figure S3). The 2015 marker year can also be linked to an especially warm and dry early summer in 2014. Similarly, the 2019 marker year follows the record-breaking dry and warm year of 2018 (Skaland et al., 2019). The significant growth decline observed one year after a drought is consistent with other studies (Lindholm et al., 2000; Andreassen et al., 2006), which attribute this pattern to previous years' growth conditions impacting the current years’ wood formation. In addition to, high cone production following warm, dry summers. Both resulting in the formation of narrower tree rings.

BAI, which accounts for diameter increment, offers a more precise measure of wood production and growth compared to Tree Ring Widths (TRW). TRW tends to narrow as trees mature despite the increasing stem diameter, requiring progressively wider rings to maintain consistency. This characteristic of TRW can potentially obscure growth trends, whereas BAI facilitates easier identification of periods with marginal growth (Labrecque et al., 2023). BAI typically increases steadily throughout a tree's lifespan, peaking as the tree matures and then plateauing, unlike TRW which generally reaches its maximum before the tree reaches ten years of age and then rapidly declines, stabilizing at a lower level (Leblanc, 1994).

The relatively young age of the sampled trees posed specific challenges in data interpretation, impacting the robustness of dendrochronological analysis for climatic interpretations. Younger stands, such as those in Elvål and Koppang, generally exhibit less stable growth patterns and, as a result, shorter overlaps in tree-ring data, which can lead to less significant statistical values (Esper et al., 2002). The variability in growth patterns among younger trees is often attributed to their immature forest structure, where the forest canopy is not yet fully established. This open canopy stage allows young trees to behave more like independent individuals rather than as part of a forest stand, potentially making them more, or less sensitive to variations in climatic factors. However, as the canopy closes and competition among trees stabilizes, these trees might begin to respond more uniformly to climatic stressors (Peters et al., 2020; Savva et al., 2003).

The study included dominant trees chosen to minimize competition and co-dominant dendrometer-fitted trees, resulting in two different diameter classes per site. When cross-dating, no significant differences were noticed between these groups, indicating similar growth trends under varying climatic influences. This consistency aligns with findings by Merian & Lebourgeois (2011), who suggested that sampling only the largest diameter Norway spruce trees is sufficient for climate-growth insights, and Meyer & Braker (2001), who found that social status had minimal impact on tree-ring climate correlations in Norway spruce. However, while I did not find substantial differences when cross-dating, I did not separate the dominant and co-dominant trees to specifically check for the strength of climate correlations.

Increasing the sample size and including a more diverse range of tree ages and social statuses could provide a more detailed understanding of these dynamics.

Comparing dominant to subdominant trees might reveal either stronger or weaker reactions to specific climatic stressors, such as droughts. Zang et al. (2012) and Bošelá et al. (2021) found that larger trees showed stronger climatic signals, supporting the importance of evaluating tree size in climate-growth studies.

5. Conclusion

This study reveals significant regional variations in climate-growth correlations for Norway spruce across a north-south gradient in southeastern Norway. It provides valuable insights into how differences in temperature and precipitation affect growth. Thus, enhancing our understanding of climate impacts on radial growth and clarifying the climatic boundaries that limit growth in boreal spruce forests, an area with limited prior research in Norway.

The results indicate a notable shift in growing conditions over the study period, characterized by a significant rise in temperatures and an extended growing season. In the North region, the strong correlation between June temperatures and BAI underscores early summer temperatures as primary growth constraints. Conversely, in the south, July precipitation significantly influences BAI, reflecting a pronounced hydrological sensitivity. The mid-region displays similar, yet less pronounced correlations compared to the south, with both previous and current summer precipitation affecting growth, highlighting the essential role of soil water availability. These results align with existing research, demonstrating that while northern regions are predominantly limited by temperature, southern regions are more influenced by precipitation.

Looking forward future research should take a more holistic approach by including analysis of soil characteristics and expanding the study to encompass different forest compositions on different soils. This broader scope will enhance our understanding of Norway spruce's resilience and its response to different climatic conditions, helping to define the boundaries between temperature and precipitation limitations more clearly. Exploring these aspects is crucial for developing effective climate adaptation strategies in forest management, ensuring the sustainability and productivity of these ecosystems in the face of climate change.

6. References

Allen, C.D., Macalady, A.K., Chenchouni, H., Bachelet, D., McDowell, N., Vennetier, M., Kitzberger, T., Rigling, A., Breshears, D.D., Hogg, E.H., Gonzalez, P., Fensham, R., Zhang, Z., Castro, J., Demidova, N., Lim, J.H., Allard, G., Running, S.W., Semerci, A. & Cobb, N. (2010). A global overview of drought and heat-induced tree mortality reveals emerging climate change risks for forests, Forest Ecology and Management, vol. 259, no. 4, pp. 660-684. https://doi.org/10.1016/j.foreco.2009.09.001

Andreassen, K., Solberg, S., Tveito, O.E., Lystad, S.L. (2006). Regional differences in climatic responses of Norway spruce (Picea abies L. Karst) growth in Norway. Forest Ecology and Management 222, 211–221. https://doi.org/10.1016/j.foreco.2005.10.029

Basler, D. & Körner, C. (2012). Photoperiod sensitivity of bud burst in 14 temperate forest tree species, Agricultural and Forest Meteorology, vol. 165, pp. 73-81. https://doi.org/10.1016/j.agrformet.2012.06.001

Bentz, B.J., Régnière, J., Fettig, C.J., Hansen, E.M., Hayes, J.L., Hicke, J.A., Kelsey, R.G., Negrón, J.F., Seybold, S.J. (2010). Climate Change and Bark Beetles of the Western United States and Canada: Direct and Indirect Effects. BioScience 60, 602–613. https://doi.org/10.1525/bio.2010.60.8.6

Bošelá, M., Sedmák, R., Sedmáková, D., Marušák, R., Kulla, L. (2014). Temporal shifts of climate–growth relationships of Norway spruce as an indicator ofhealth decline in the Beskids. Slovakia. For. Ecol. Manage. 325, 108–117. https://doi.org/10.1016/j.foreco.2014.03.055

Bošelá, M., Tumajer, J., Cienciala, E., Dobor, L., Kulla, L., Marčiš, P., Popa, I., Sedmák, R., Sedmáková, D., Sitko, R., Šebeň, V., Štěpánek, P., Büntgen, U. (2021). Climate warming induced synchronous growth decline in Norway spruce populations across biogeographical gradients since 2000. Science of The Total Environment 752, 141794. https://doi.org/10.1016/j.scitotenv.2020.141794

Bradshaw, C.J.A. & Warkentin, I.G. (2015). Global estimates of boreal forest carbon stocks and flux, Global and Planetary Change, vol. 128, pp. 24-30. http://dx.doi.org/10.1016/j.gloplacha.2015.02.004

Bunn, A., Korpela, M., Biondi, F., Campelo, F., Mérian, P., Qeadan, F., Zang, C. (2020). dplR: dendrochronology program library in R. R Package Version 1.7.6. Available at: https://github.com/AndyBunn/dplR

Bunn, A.G., Jansma, E., Korpela, M., Westfall, R.D. & Baldwin, J. (2013). Using simulations and data to evaluate mean sensitivity (ζ) as a useful statistic in dendrochronology. Dendrochronologia, vol. 31, no. 3, pp. 250-254. https://doi.org/10.1016/j.dendro.2013.01.004

Buras, A., 2017. A comment on the expressed population signal. Dendrochronologia 44, 130–132. https://doi.org/10.1016/j.dendro.2017.03.005

Čermák, P., Rybníček, M., Žid, T., Andreassen, K., Børja, I., Kolář, T. (2017). Impact of climate change on growth dynamics of Norway spruce in south-eastern Norway. Silva Fennica vol. 51 no. 2 article id 1781. https://doi.org/10.14214/sf.1781

Čermák, P., Rybníček, M., Žid, T., Steffenrem, A., Kolář, T. (2019). Site abd age-dependance of Picea abies growth to climate variability. European Journal of Forest Research 138(3):445–460. https://doi.org/10.1007/s10342-019-01182-6

D'Andrea, G., Šimůnek, V., Pericolo, O., Vacek, Z., Vacek, S., Corleto, R., Olejár, L., Ripullone, F. (2023). Growth Response of Norway Spruce (Picea abies [L.] Karst.) in Central Bohemia (Czech Republic) to Climate Change. Forests 2023, 14, 1215. https://doi.org/10.3390/f14061215

De Frenne, P., Graae, B.J., Rodríguez-Sánchez, F., Kolb, A., Chabrerie, O., Decocq, G., De Kort, H., De Schrijver, A., Diekmann, M., Eriksson, O., Gruwez, R., Hermy, M., Lenoir, J., Plue, J., Coomes, D.A., Verheyen, K. (2013). Latitudinal gradients as natural laboratories to infer species' responses to temperature. Journal of Ecology 101, 784–795. https://doi.org/10.1111/1365-2745.12074

Esper, J., Cook, E.R., and Schweingruber, F.H. (2002). Low-frequency signals in long tree-ring chronologies for reconstructing past temperature variability. Science, vol. 295, no. 5563, pp. 2250-2253. https://doi.org/10.1126/science.1066208

ETCCDI. (2009). Climate Change Indices: Definitions of the 27 core indices. http://etccdi.pacificclimate.org/list_27_indices.shtml

Frich, P., Alexander, L., Della-Marta, P., Gleason, B., Haylock, M., Klein Tank, A. and Peterson, T. (2002). Observed coherent changes in climatic extremes during the second half of the twentieth century. Climate Research, 19, 193–212. doi:10.3354/cr019193

Fritts, H.C. (1976). Tree ring and climate. Academic Press, London, New York, San Francisco.

Gohli, J., Krokene, P., Heggem, E.S.F., Økland, B. (2024). Climatic and management-related drivers of endemic European spruce bark beetle populations in boreal forests. Journal of Applied Ecology. 61. http://dx.doi.org/10.1111/1365-2664.14606

Griesbauer, H., DeLong, S.C., Rogers, B. et al. (2021). Growth sensitivity to climate varies with soil moisture regime in spruce–fir forests in central British Columbia. Trees 35, 649–669. https://doi.org/10.1007/s00468-020-02066-8

Grundmann, B.M., Bolte, A., Bonn, S. & Roloff, A. (2011). Impact of climatic variation on growth of Fagus sylvatica and Picea abies in Southern Sweden. Scandinavian Journal of Forest Research, vol. 26, no. S11, pp. 64-71. https://doi.org/10.1080/02827581.2011.564392

Hanssen-Bauer, I., Førland, E.J., Haddeland, I., Hisdal, H., Mayer, S., Nesje, A., Nilsen, J.E.Ø., Sandven, S., Sandø, A.B., Sorteberg, A., Ådlandsvik, B. (2015). Climate in Norway 2100–Knowledge base for climate adaptation, updated in 2015. Norwegian Centre for Climate Services. pp 203

Hartmann, H., Bastos, A., Das, A.J., Esquivel-Muelbert, A., Hammond, W.M., Martínez-Vilalta, J., McDowell, N.G., Powers, J.S., Pugh, T.A.M., Ruthrof, K.X., Allen, C.D. (2022). Climate Change Risks to Global Forest Health: Emergence of Unexpected Events of Elevated Tree Mortality Worldwide. Annu Rev Plant Biol. 73:673-702. https://doi.org/10.1146/annurev-arplant-102820-012804

Hlásny, T., König, L., Krokene, P., Lindner, M., Montagné-Huck, C., Müller, J., Qin, H., Raffa, K.F., Schelhaas, M.-J., Svoboda, M., Viiri, H., Seidl, R. (2021). Bark Beetle Outbreaks in Europe: State of Knowledge and Ways Forward for Management. Curr Forestry Rep 7, 138–165. https://doi.org/10.1007/s40725-021-00142-x

Kausrud, K., Vandvik, V., Flø, D., Geange, S.R., Hegland, S.J., Hermansen, J.S., Hole, L.R., Ims, R.A., Kauserud, K., Kirkendall, L.R., Nordén, J., Nybakken, L., Ohlson, M., Skarpaas, O. (2022). Impacts of climate change on the forest ecosystem. Scientific Opinion of the Panel on Alien Organisms and Trade in endangered species (CITES) of the Norwegian Scientific Committee for Food and Environment. VKM Report 2022:15, ISBN: 978-82-8259-390- 8, ISSN: 2535-4019. Norwegian Scientific Committee for Food and Environment (VKM), Oslo, Norway

Larsson, L. (2013). C-Dendro, Cybis Elektronik & Data AB. Available at: http://www.cybis.se/forfun/dendro/

Labrecque-Foy, J.-P., Angers-Blondin, S., Ropars, P., Simard, M., Boudreau, S. (2023). The Use of Basal Area Increment to Preserve the Multi-Decadal Climatic Signal in Shrub Growth Ring Chronologies: A Case Study of Betula glandulosa in a Rapidly Warming Environment. Atmosphere 14, 319. https://doi.org/10.3390/atmos14020319

LeBlanc, D.C. (1994). Using Tree Rings to Study Forest Decline: An Epidemiological Approach Based on Estimated Annual Wood Volume Increment. In Proceedings of the Tree Rings, Environment and Humanity, Tucson, AZ, USA, 17–21 May 1994; pp. 437–449.

Lie, M.H., Asplund, J., Göhl, M., Ohlson, M., Nybakken, L. (2023). Similar growth responses to climatic variations in Norway spruce (Picea abies) and European beech (Fagus sylvatica) at the northern range limit of beech. Eur J Forest Res 142, 1059–1068. https://doi.org/10.1007/s10342-023-01576-7

Lindner, M., Maroschek, M., Netherer, S., Kremer, A., Barbati, A., Garcia-Gonzalo, J., Seidl, R., Delzon, S., Corona, P., Kolström, M., Lexer, M.J., & Marchetti, M. (2010). Climate change impacts, adaptive capacity, and vulnerability of European forest ecosystems. Forest Ecology and Management, vol. 259, no. 4, pp. 698-709. https://doi.org/10.1016/j.foreco.2009.09.023

Lindholm M., Lehtonen H., Kolström T., Meriläinen J., Eronen M., Timonen M. (2000). Climatic signals extracted from ring-width chronologies of Scots pines from the northern, middle and southern parts of the boreal forest belt in Finland. Silva Fennica vol. 34 no. 4 article id 616. https://doi.org/10.14214/sf.616

Lussana, C., Saloranta, T., Skaugen, T., Magnusson, J., Tveito, O.E. & Andersen, J. (2018). seNorge2 daily precipitation, an observational gridded dataset over Norway from 1957 to the present day. Earth System Science Data, vol. 10, pp. 235-249. https://doi.org/10.5194/essd-10-235-2018

Lutz, J., Hanssen-Bauer, I., Tveito, O.E., Dobler, A. (2024). Precipitation variability in Norway 1961-2020. Norwegian Meteorological Institute. MET Report No. 1/2024. ISSN 2387-4201.

Lyu, L., Suvanto, S., Nöjd, P., Henttonen, H.M., Mäkinen, H., Zhang, Q.-B. (2017). Tree growth and its climate signal along latitudinal and altitudinal gradients: comparison of tree rings between Finland and the Tibetan Plateau. Biogeosciences 14, 3083–3095. https://doi.org/10.5194/bg-14-3083-2017

Mäkinen, H., Nöjd, P., Kahle, H.-P., Neumann, U., Tveite, B., Mielikäinen, K., Röhle, H., Spiecker, H. (2002). Radial growth variation of Norway spruce (Picea abies (L.) Karst.) across latitudinal and altitudinal gradients in central and northern Europe. Forest Ecology and Management 171, 243–259. https://doi.org/10.1016/S0378-1127(01)00786-1

Menzel, A. (1997). Phänologie von Waldbäumen unter sich ändernden Klimabedingungen - Auswertung der Beobachtungen in den Internationalen Phänologischen Gärten und Möglichkeiten der Modellierung von Phänodaten. Forstliche Forschungsberichte München.

Mérian, P., Lebourgeois, F. (2011). Size-mediated climate-growth relationships in temperate forests: a multi-species analysis. Forest Ecology and Management 261(8): 1382–1391. https://doi.org/10.1016/j.foreco.2011.01.019.

Meyer, F.D., Braker, O.U. (2001). Climate response in dominant and suppressed spruce trees Picea abies (L.) Karst., on a subalpine and lower montane site in Switzerland. Ecoscience 8, 105–114. https://doi.org/10.1080/11956860.2001.11682636

Moen, A. (1999) Atlas of Norway. Vegetation, Norwegian Mapping Authority, Hønefoss

Netherer, S., Hammerbacher, A. (2022). The Eurasian spruce bark beetle in a warming climate: phenology, behavior, and biotic interactions. In: Gandhi, K.J.K., Hofstetter, R.W. (Eds.), Bark Beetle Management. Ecology, and Climate Change. http://dx.doi.org/10.1016/B978-0-12-822145-7.00011-8

Netherer, S., Lehmanski, L., Bachlehner, A., Rosner, S., Savi, T., Schmidt, A., Huang, J., Paiva, M.R., Mateus, E., Hartmann, H., Gershenzon, J. (2024). Drought increases Norway spruce susceptibility to the Eurasian spruce bark beetle and its associated fungi. New Phytologist 242, 1000–1017. https://doi.org/10.1111/nph.19635

Nuske, R. (2022). vegperiod: Determine Thermal Vegetation Periods. R package version 0.4.0. Available at: https://github.com/rnuske/vegperiod

Pan, Y., Birdsey, R.A., Fang, J., Houghton, R., Kauppi, P.E., Kurz, W.A., Phillips, O.L., Shvidenko, A., Lewis, S.L., Canadell, J.G., Ciais, P., Jackson, R.B., Pacala, S.W., McGuire, A.D., Piao, S., Rautiainen, A., Sitch, S., Hayes, D.

(2011). A Large and Persistent Carbon Sink in the World's Forests. Science 333, 988–993. https://doi.org/10.1126/science.1201609
Peters, R.L., Groenendijk, P., Vlam, M., & Zuidema, P.A. (2015). Detecting long-term growth trends using tree rings: A critical evaluation of methods. Global Change Biology, vol. 21, pp. 2040-2054. https://doi.org/10.1111/gcb.12826
Pirtskhalava-Karpova, N., Trubin, A., Karpov, A., Jakuš, R. (2024). Drought initialised bark beetle outbreak in Central Europe: Meteorological factors and infestation dynamic. Forest Ecology and Management 554, 121666. https://doi.org/10.1016/j.foreco.2023.121666
Popa A., Popa I., Roibu C-C., Badea O, N. (2022). Do Different Tree-Ring Proxies Contain Different Temperature Signals? A Case Study of Norway Spruce (Picea abies (L.) Karst) in the Eastern Carpathians. Plants. 2022; 11(18):2428. https://doi.org/10.3390/plants11182428
R Core Team. (2023). R: A language and environment for statistical computing. R Foundation for Statistical Computing, Vienna, Austria. Available at: https://www.R-project.org/
Savva, Y., Oleksyn, J., Reich, P.B., Tjoelker, M.G., Vaganov, E.A. & Modrzynski, J. (2006). Interannual growth response of Norway spruce to climate along an altitudinal gradient in the Tatra Mountains, Poland. Trees, vol. 20, pp. 735-746. http://dx.doi.org/10.1007/s00468-006-0088-9
Skaland, R, G., Collueuille, H., Andersen, A, S, H., Mamen, J., Grinde, L, et al. (2019). Tørkesommeren 2018. Meterologisk institutt. METinfo No. 14/2019. ISSN 1894-759X.
Speer, J.H. (2010). Fundamentals of Tree-ring Research. University of Arizona Press, Tucson.
Voelker, S.L. (2011). Age-dependent changes in environmental influences on tree growth and their implications for forest responses to climate change. In: Meinzer F.C., Lachenbruch B., Dawson T.E. (eds.). Size- and age-related changes in tree structure and function. Tree physiology 4: 455–479. https://doi.org/10.1007/978-94-007-1242-3_17.
von Wilpert, K. (1990). Die Jahrringstruktur von Fichten in Abhängigkeit vom Bodenwasserhaushalt auf Pseudogley und Parabraunerde: Ein Methodenkonzept zur Erfassung standortsspezifischer Wasserstreßdispostion. Freiburger Bodenkundliche Abhandlungen.
Walther, A. and Linderholm, H. W. (2006). A comparison of growing season indices for the Greater Baltic Area. International Journal of Biometeorology, 51(2), 107–118. https://doi.org/10.1007/s00484-006-0048-5
Wigley, T.M.L., Briffa, K.R. & Jones, P.D. (1984). On the average value of correlated time series, with applications in dendroclimatology and hydrometeorology. Journal of Climate and Applied Meteorology, vol. 23, pp. 201-213.https://doi.org/10.1175/1520-0450(1984)023%3C0201:OTAVOC%3E2.0.CO;2

Zang, C., Pretzsch, H., Rotne, R. (2012). Size-dependent responses to summer drought in Scots pine, Norway spruce and common oak. Trees 26, 557-569. https://doi.org/10.1007/s00468-011-0617-z

Zang, C. & Biondi, F. (2022). treeclim: Numerical Calibration of Proxy-Climate Relationships. R package version 2.0.6.0. Available at: https://github.com/cszang/treeclim

Zhang, X., Alexander, L., Hegerl, G. C., Jones, P., Tank, A. K., Peterson, T. C., Trewin, B. and Zwiers, F. W. (2011). Indices for monitoring changes in extremes based on daily temperature and precipitation data. Wiley Interdisciplinary Reviews: Climate Change, 2(6), 851–870. https://doi.org/10.1002/wcc.147

7. Appendix

7.1 Supplementary figures

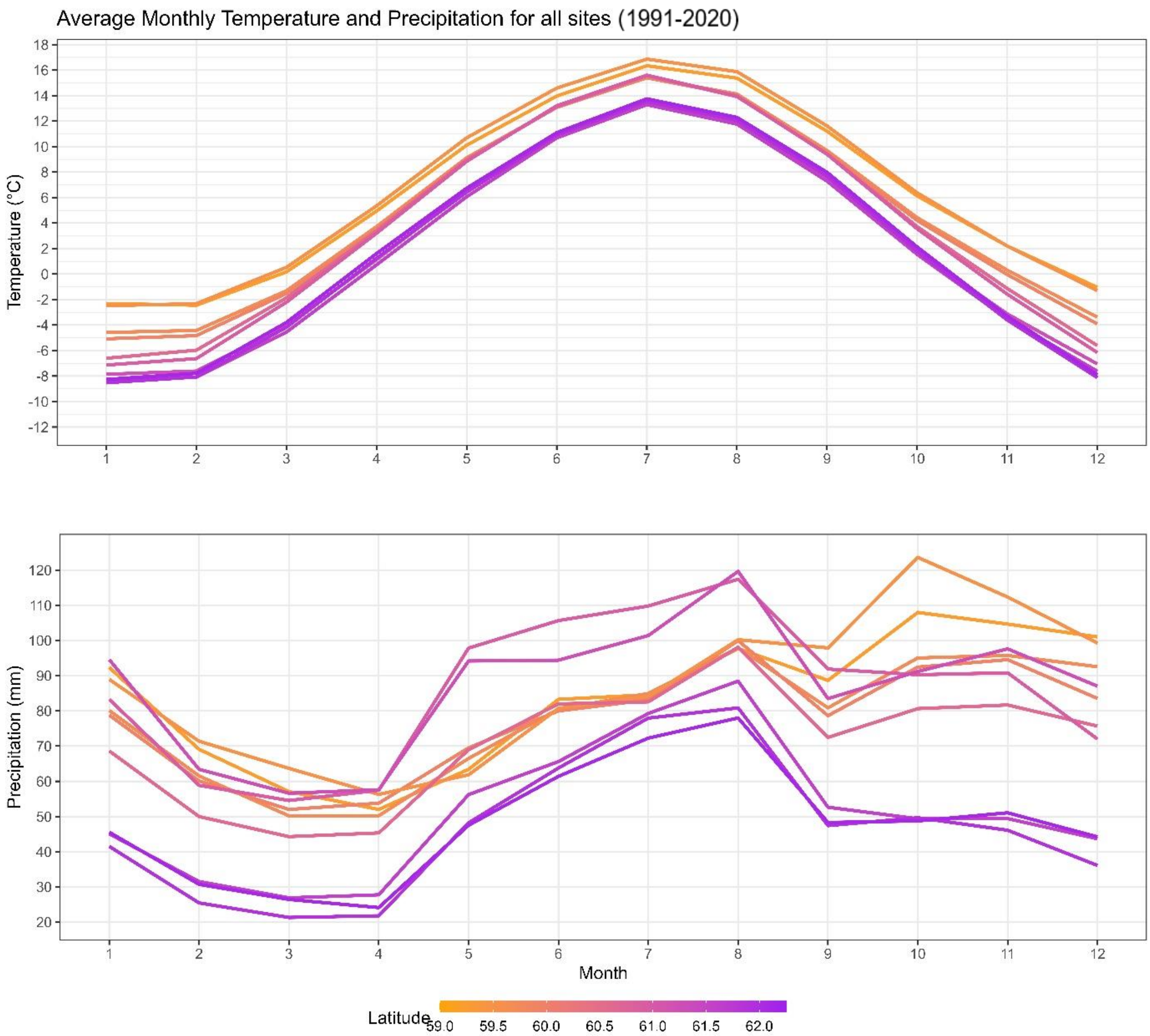

Figure S1. Average monthly temperature (top) and precipitation (bottom) for the period 1991-2022 for all sites, coloured by latitude.

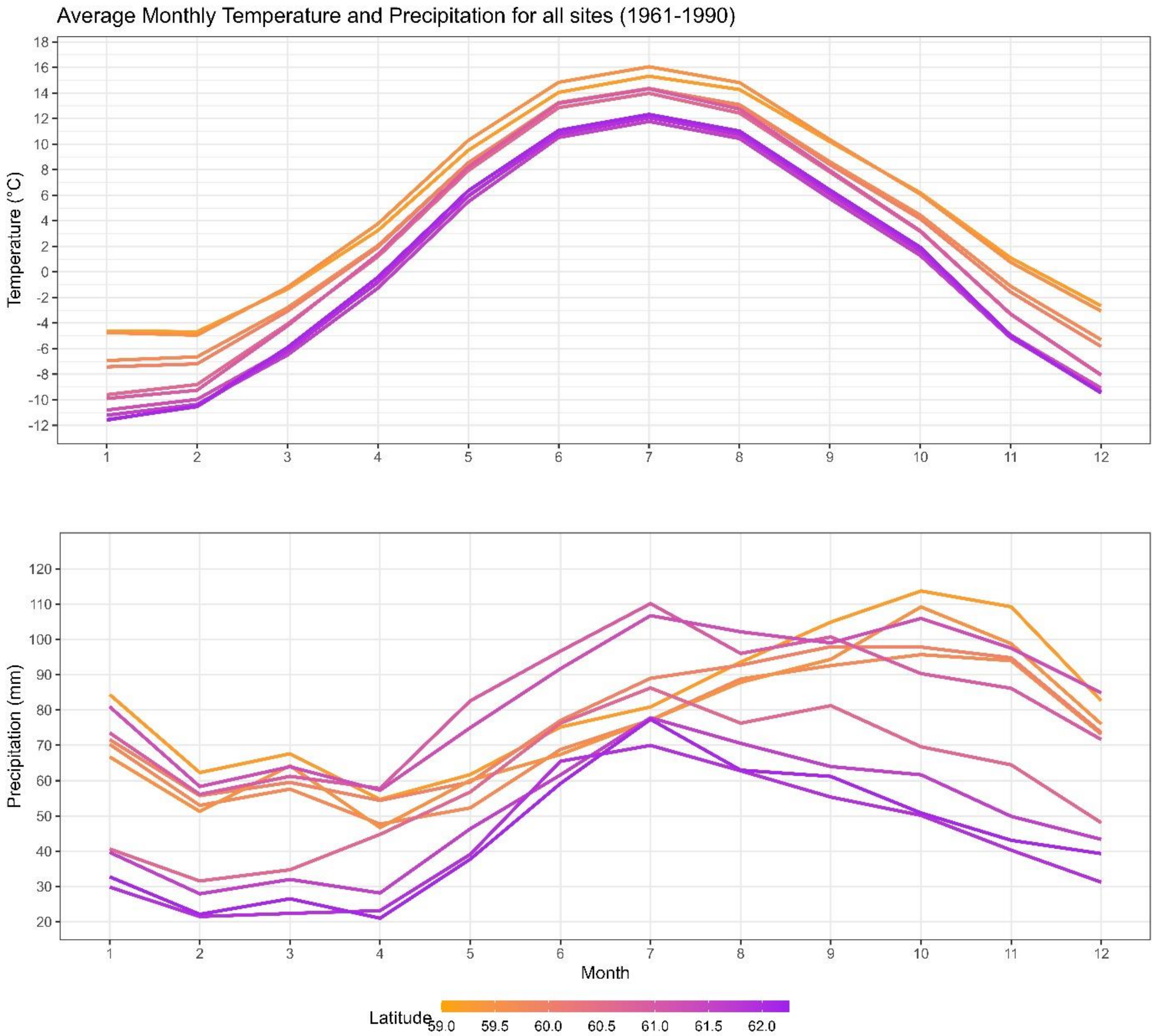

Figure S2. Average monthly temperatures (top) and precipitation (bottom) for the period 1961-1990 for all sites, coloured by latitude.

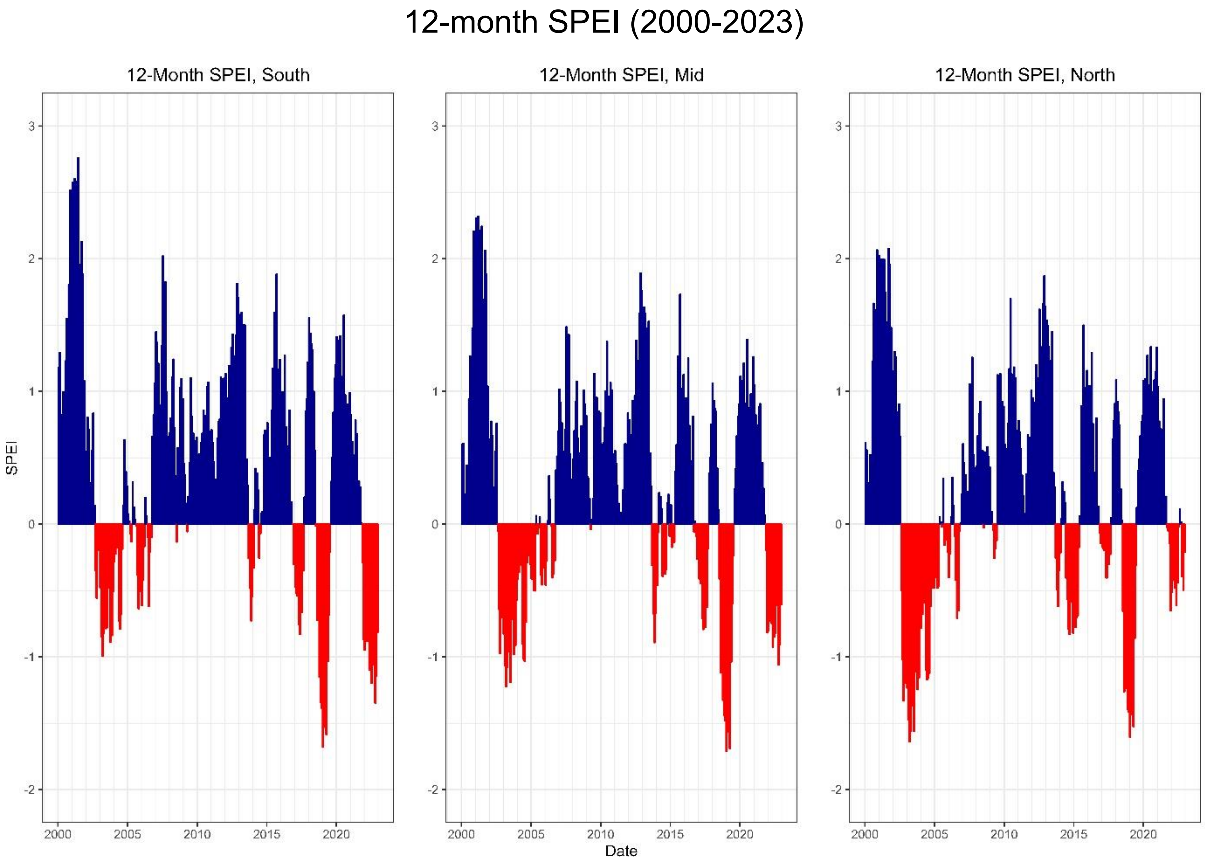

Figure S3. 12-month Standardized Precipitation-Evapotranspiration Index SPEI for the three regions South, Mid, and North (Dataset: SPEIbase v.2.9). Blue areas represent positive SPEI, indicating wetter than average conditions and red areas represent negative SPEI, indicating drier than average conditions for the previous 12 month period.

Monthly Growth- Temperature correlations for all sites except Finnstad

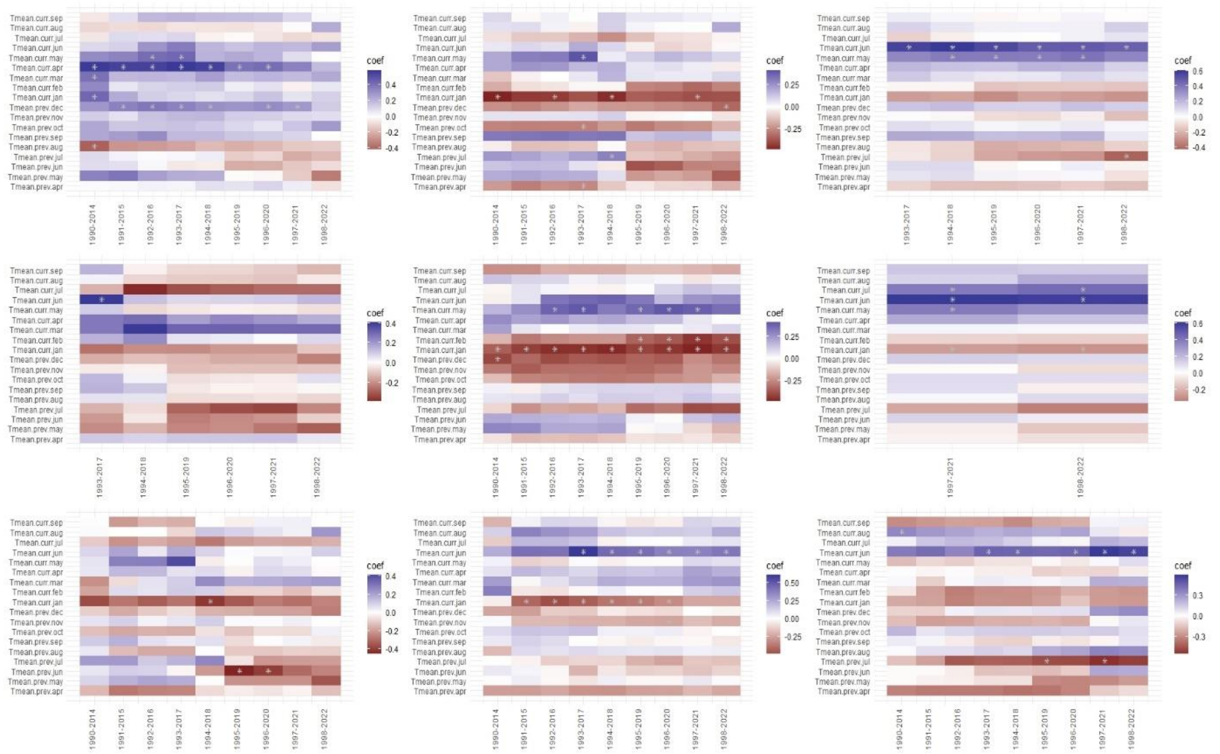

Figure S4. Heatmap illustrating correlation between monthly mean temperature for all sites through time. From current September until previous April. Red colours indicate negative correlations, while blue indicate positive. Asterisks denote statistical significance. Plots 1, 7, 3 are displayed on the left side, 5, 9, 11 in the middle and 13, 15, 19 on the right side. Plot 17 was excluded because of the young age of the stand.

Monthly Growth- Precipitation correlations for all sites except Finnstad

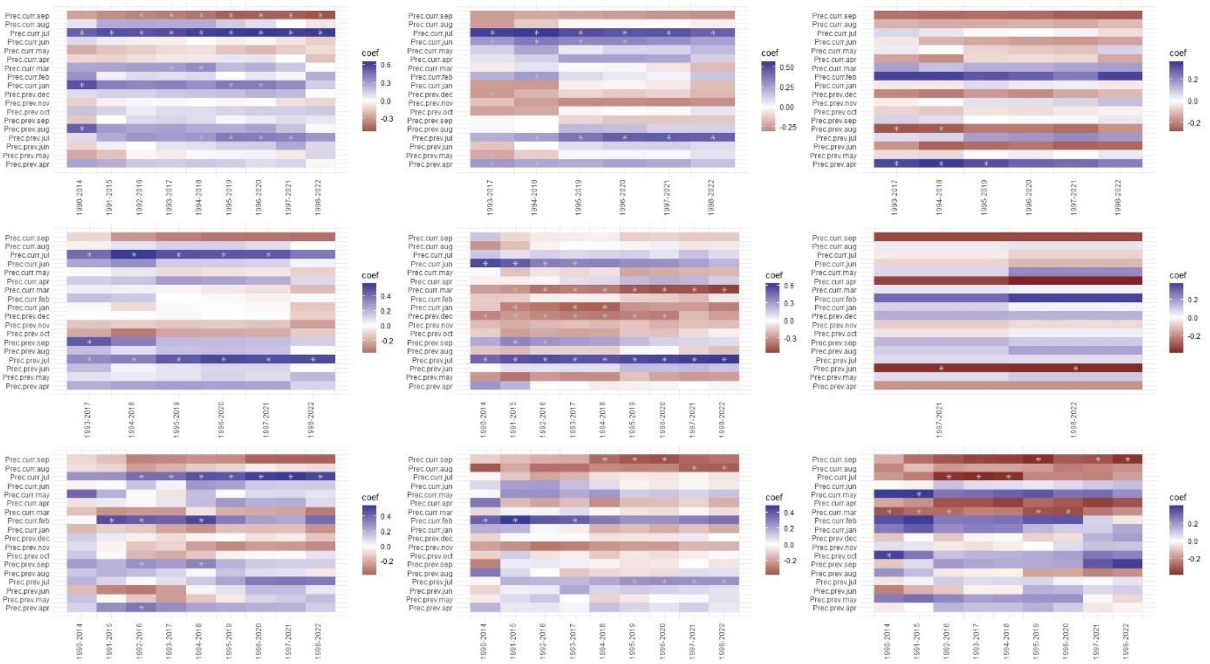

Figure S5. Heatmap illustrating correlation between monthly precipitation sums for all sites trough time. From current September until previous April. Red colours indicate negative correlations, while blue indicate positive. Asterisks denote statistical significance. Plots 1, 7, 3 are displayed on the left side, 5, 9, 11 in the middle and 13, 15, 19 on the right side. Plot 17 was excluded because of the young age of the stand.

Norges miljø- og biovitenskapelige universitet
Noregs miljø- og biovitskapelege universitet
Norwegian University of Life Sciences

Postboks 5003
NO-1432 Ås
Norway